Available online at www.sciencedirect.com
SCIENCE DIRECT®

Journal of the European Ceramic Society 24 (2004) 111–117

www.elsevier.com/locate/jeurceramsoc

Production of rare-earth orthoferrite ceramic fibres by aqueous sol-gel blow spinning process

M. Rajendran, A.K. Bhattacharya*

Warwick Process Technology Group, School of Engineering, University of Warwick, Coventry CV4 7AL, UK

Received 8 December 2002; received in revised form 9 March 2003; accepted 15 March 2003

Abstract

Rare-earth orthoferrite, $LnFeO_3$ (Ln = La, Sm, Gd, Dy, Er and Yb) ceramic fibres were produced by aqueous sol-gel blow spinning process at low-temperatures. Stable, charge stabilised, colloidal precursor sols of orthoferrites were prepared by room temperature processing of inexpensive and commercially available metal salts. The average diameter (Z_{av}) of the colloidal sol particles was in the range 4–7 nm and had a narrow size distribution. The sols were concentrated, combined with spinning aids, and processed further to a viscous 'spinning solution'. The gel fibres of about 6 μm diameter were blow spun, collected as random fibres, dried and heated to increasingly higher temperatures at a rate of 50 °C/h. The gel fibres converted to flexible ceramic fibres, and single-phase perovskite structure crystallised directly for all the $LnFeO_3$ (Ln = La, Sm, Gd, Dy, Er and Yb) fibres on heating them to 700 °C. The ceramic fibres had mean diameter of about 3–4 μm, and consisted of randomly oriented submicron sized grains.

Keywords: Blow spinning; Fibres; $LnFeO_3$; Orthoferrite fibres; Sol-gel process

1. Introduction

The rare earth orthoferrites ($LnFeO_3$ where, Ln = rare earth) are a class of materials having potential for various applications. These compounds and metal ion substituted ferrites crystallising in perovskite structure show promise as catalysts,[1] gas separators,[2,3] cathodes in solid oxide fuel cells,[4] sensor materials,[5] magneto-optic materials [6] and as spin valves.[7] The earlier studies on orthoferrites are confined to powders, sintered components and films. There is a growing interest to study complex oxide materials in the fibrous form, because in this form the fine grain features are maintained, the material is easy to handle, grains can be preferentially aligned, and the brittleness inherent to ceramics could be remarkably reduced. In addition, complex shapes and forms can be fabricated using fibres, enhanced mechanical and electromagnetic properties obtained, and newer applications could be explored. Especially, composites reinforced with ceramic fibres and whiskers are of special interest for various structural and technological applications.

Normally, in sol-gel process metal alkoxides or heterometal alkoxides are dissolved in alcohol and hydrolysed under controlled conditions to produce a sol.[8,9] The sol is processed further to produce fine powders, thin films and fibres. However, use of metal alkoxides and organic solvents are process intensive in view of recovery and re-use of solvents, storage and handling of chemicals. In addition, the cost of chemicals makes the process suitable only for speciality applications, small scale preparations and exploratory work. As an alternative, we have been exploring inexpensive aqueous sol-gel process to produce ceramic powders, thin films and fibres.[10–14] The ceramics in fibrous form are of interest since the brittleness associated with bulk materials could be overcome to a large extent. In addition, the electrical and magnetic properties of these materials in the fibrous form would be different to that of the bulk ceramics. However, there has been no report available in the literature on the production of perovskite structured orthoferrite fibres. Therefore, we report an aqueous sol-gel process to produce orthoferrite ceramic fibres, and provide results on the thermal evolution of crystal structure.

* Corresponding author. Tel.: +44-2476-524-201; fax: +44-2476-528-998.
E-mail address: akb@warwick.ac.uk (A.K. Bhattacharya).

0955-2219/03/$ - see front matter © 2003 Elsevier Ltd. All rights reserved.
doi:10.1016/S0955-2219(03)00267-X

1.1. Experimental methods

A 200 ml of 0.2 M aqueous solution of lanthanum nitrate, $La(NO_3)_3.9H_2O$ (99.99%, Aldrich) was mixed with 200 ml of 0.2 M iron(III) nitrate, $Fe(NO_3)_3.9H_2O$ (99.99+%, Aldrich) and titrated with 5% aqueous ammonia solution with constant stirring (300 rpm) at room-temperature until complete precipitation of lanthanum and iron as mixed hydroxides. The precipitate was filtered, washed with water and peptised to get a clear sol.[8] The resultant sol was centrifuged at 4000 rpm for 15 min to eliminate traces of residual precipitates. The sol was concentrated under a reduced pressure (10^{-2} torr) at room temperature to a viscous sol containing 25 wt.% solid, blended with polyethylene oxide solution (2 wt.%) and concentrated to 30–35 wt.% solid dispersion. The resultant 'spinning solution' was blow spun to produce gel fibres using a proprietary spinning unit. The gel fibres were collected as random fibres, dried at 100 °C, heated to higher temperatures at a rate of 50–75 °C/h. The other rare-earth ferrite fibres were produced following the same procedure but using stoichiometric amount of corresponding rare-earth nitrates instead of lanthanum nitrate.

The sols were characterised for their particle size and size distribution using CONTIN method on a photon correlation spectrometer (PCS), Malvern Instruments, Lo-C Autosizer, series 7032 multi 8-correlator, using a 4 mW diode laser, operating at a wavelength of 670 nm. The crystallinity, crystal structure and phase composition of the fibres were charaterised by Philips X-ray diffractometer model PW1710 using CuK_α radiation. The spectra were recorded in the region of $2\theta = 10$–$90°$ with a step scan of 0.1° per minute and the cell parameters were calculated and further refined using linear regression procedures (Philips APD 1700 software).

Simultaneous TG-DTA analysis was performed on gel fibres of about 20 mg quantity using a Rheometric Scientific STA 1500 in flowing air up to 1000 °C at a rate of 10 °C. Scanning electron microscopic (SEM) analysis of the fibres was performed using a Cambridge Instruments Stereoscan 90 SEM operating at 15 kV. Fibres were gold coated by sputtering prior to SEM analysis rendering them electrically conductive. The fibre diameter, and microstructure details were obtained from these studies. Optical microscopy was also used to examine the length distribution of fibres.

1.1.1. Results and discussion

For all samples the size of sol particles varied between 4 and 7 nm and the average size (Z_{av}) was about 6 nm. PCS spectra of $LnFeO_3$ (Ln = La, Sm, Gd and Yb) precursor sols are shown in Fig. 1. It is clearly seen from the spectra that the size distribution falls well within the narrow range of 4–7 nm with Z_{av} of 6.3 nm. The dilute sols of 30 g hydrous metal oxide/litre concentrations were stable for over a period of few weeks as inferred from *PCS* measurements as the spectrum remained unchanged. Similar results were obtained for all the orthoferrite precursor sols and the corresponding Z_{av}

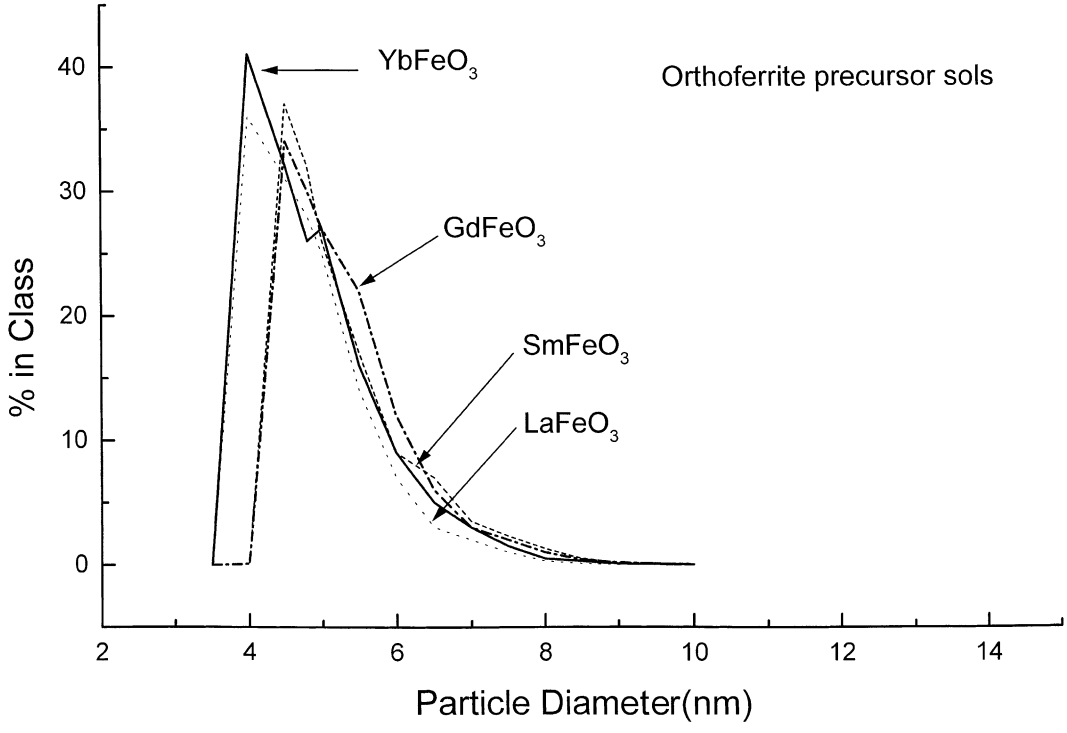

Fig. 1. Photon correlation spectrum of $LnFeO_3$ (La = La, Sm, Gd and Yb) precursor sols.

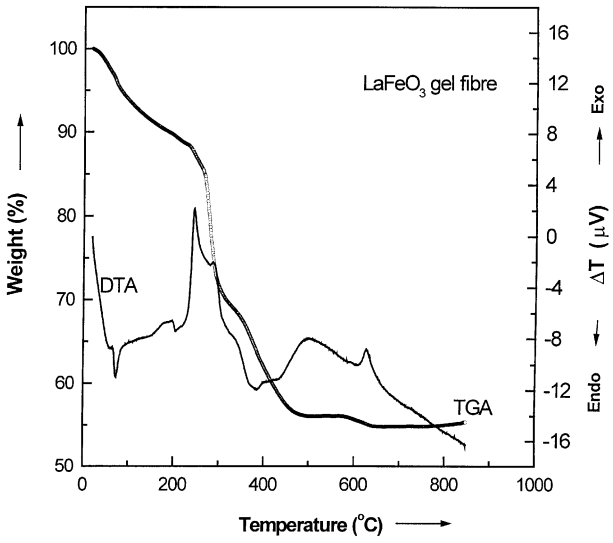

Fig. 2. TG-DTA curve of a typical $LaFeO_3$ gel fibre heated in static air.

values are listed in Table 1. The pH of the sols were in the range 3.7–4.3, and addition of electrolytes or any change in pH beyond this range destabilised these electrostatically charge stabilised colloidal sol particles. The viscosity of the sol increased on concentration, spinnability was bestowed with the addition of a small amount of spinning aid, polyethylene oxide (2 wt.% poly-ox) solution. However, the 'poly-ox' addition destabilised the sols, reduced the shelf-life to only few days, and the spinning was, therefore, carried out within a day or two.

Table 1
The particle sizes of the precursor sols and the unit cell parameters of the orthoferrite fibres heated to 700 °C for 2h

Compound	Sol particle size(nm)	Unit cell parameters (Å)		
		a	*b*	*c*
$LaFeO_3$	6.3	5.552	5.563	7.862
$SmFeO_3$	6.0	5.392	5.591	7.713
$GdFeO_3$	6.0	5.345	5.614	7.669
$DyFeO_3$	5.8	5.301	5.598	7.623
$ErFeO_3$	5.5	5.263	5.584	7.595
$YbFeO_3$	5.6	5.233	5.557	7.572

The 'spinning solution' was extruded through a row of cylindrical pores (280 μm pore diameter and 1200 μm pore length), on either side of which parallel jets of humidified air was flown continuously. A secondary stream of hot air was flown to complete the gelation process, and to assist partial drying of the fibres. Incomplete gelation and excess moisture resulted in deformation, twisting and sticking of gel fibres to one another to form web-like features. Therefore, the spinning conditions were optimised to produce nearly uniform, equi-diameter gel fibres. The fibres were produced at a rate of 8–9 m s^{-1}. The temperature in the chamber was at about 60 °C, and the fumes were continuously

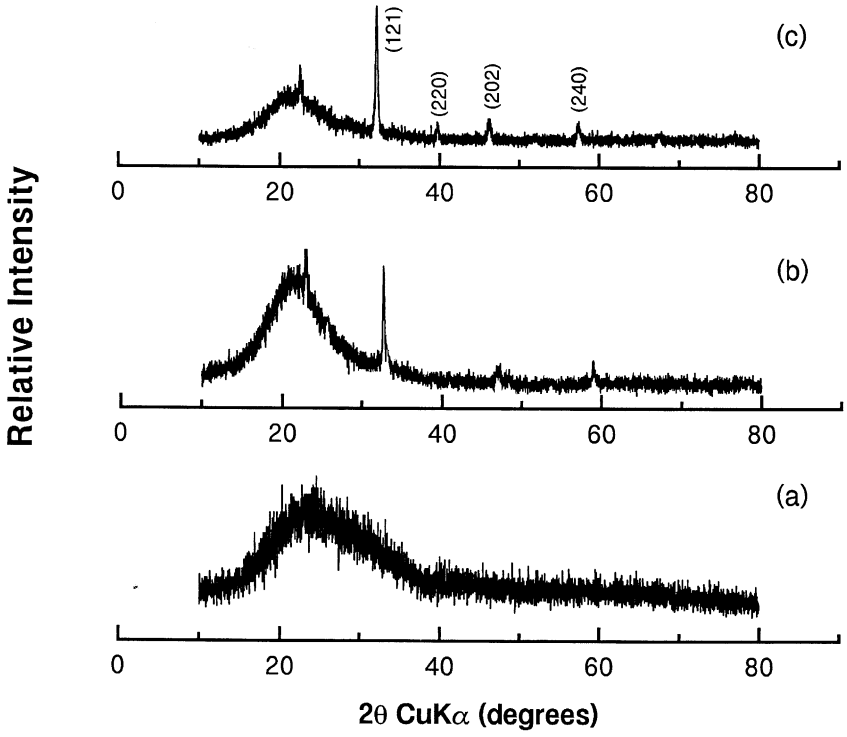

Fig. 3. Typical powder X-ray diffraction patterns of $LaFeO_3$ gel fibre heated to (a) 500 °C, (b) 650 °C and (c) 700 °C, mounted on quartz plates. The broad 'halo' in the $2\theta = 15–25°$ is from the quartz plate.

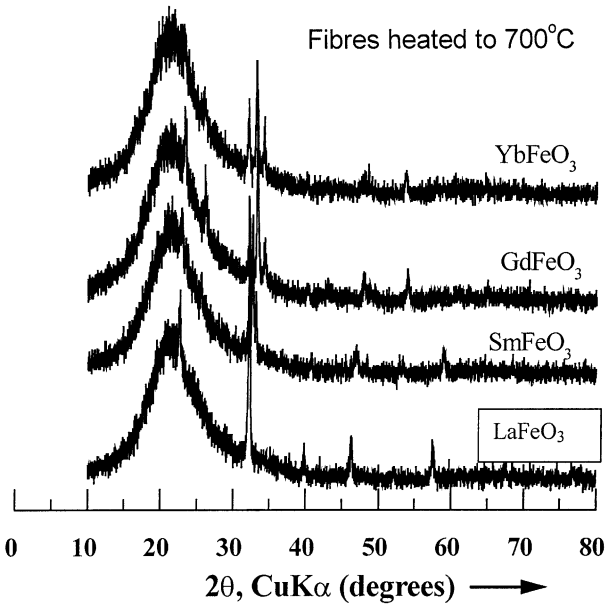

Fig. 4. Powder XRD patterns of fibres heated to 700 °C, and mounted on quartz plates for measurements. The broad feature in the $2\theta = 15$–$25°$ corresponds to the quartz plate.

extracted from the chamber. The resultant gel fibres were collected, dried and stored in a oven set at 100 °C.

Simultaneous TG-DTA trace of oven dried $LaFeO_3$ precursor gel fibre in static air at a heating rate of 10 °C is shown in Fig. 2. As seen from the thermo-gram, the TG curve shows three main weight-loss steps corresponding to (a) dehydration of water from the gel (b) oxidation of 'poly-ox' followed by de-hydroxylation of structural hydroxy groups, and (c) decomposition of residual, surface bound groups with subsequent crystallisation of $LaFeO_3$. The DTA curves show one to one correspondence with the TG weight-loss steps. The dehydration process is resolved into three events with a sharp endotherm centred around 90 °C in DTA. The 'poly-ox' decomposition is shown up as broad exotherms centered around 220 and 285 °C. Subsequent dehydroxylation reaction is seen as a broad endotherm around 400 °C. A stable weight-loss step is found in the temperaure region 470–570 °C and a constant weight is registered eventually at 650 °C. However, about 2 wt.% of residual decomposable matter or entrapped gases were retained at this stage, which is completely lost at 620 °C. The exotherm at 620 °C is attributed to the crystallisation of the perovskite structure. However, isothermally heated fibres showed constant weight at 500 °C and above, and the heated fibres were X-ray amorphous or poorly crystalline below 600 °C. Therefore, the fibres were heated to increasingly higher temperatures to induce crystallisation, and select temperatures were chosen accordingly to anneal the fibres.

The $LaFeO_3$ fibres were heated to (a)500, (b) 650 and (c) 700 °C, ground and mounted on quartz plates for XRD measurements, and the typical powder XRD patterns are shown in Fig. 3. Fig. 3(a) reveals the predominantly amorphous nature of the fibres heated to 500 °C.

The broad halo seen in the $2\theta = 15$–$25°$ is characteristic of the quartz plate used to mount the fibre sample for XRD measurement. On heating to higher temperatures, the fibre crystallises partially at 650 °C as shown

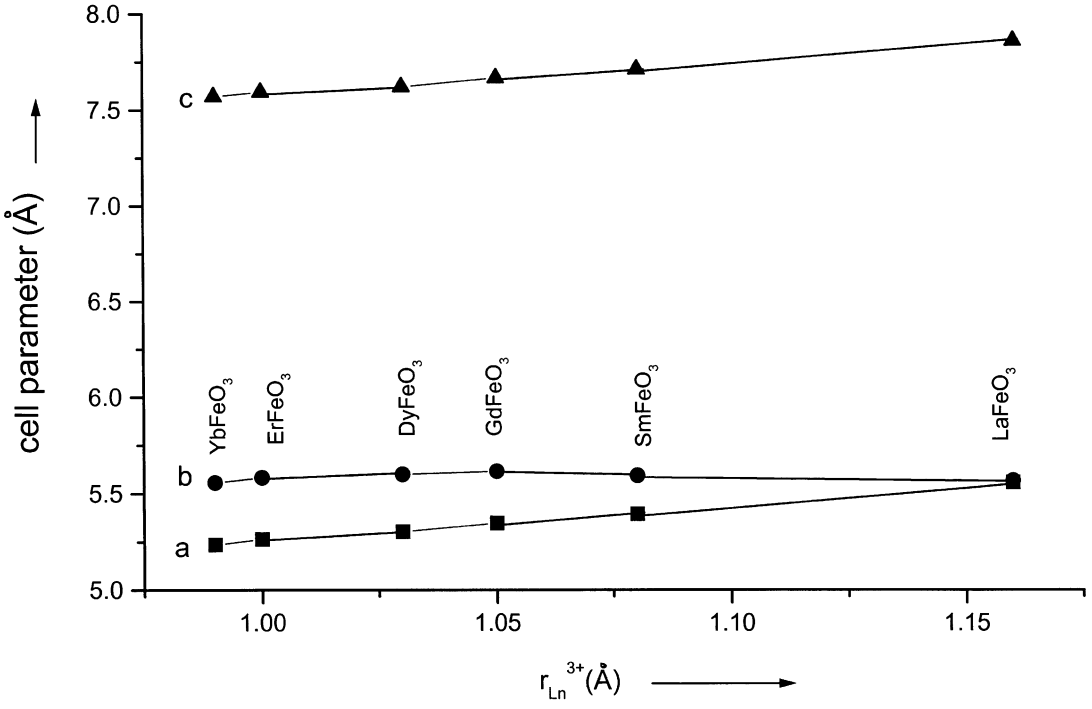

Fig. 5. Unit cell parameters of orthoferrite fibres against the radius of rare-earth ion in eight-fold coordination.

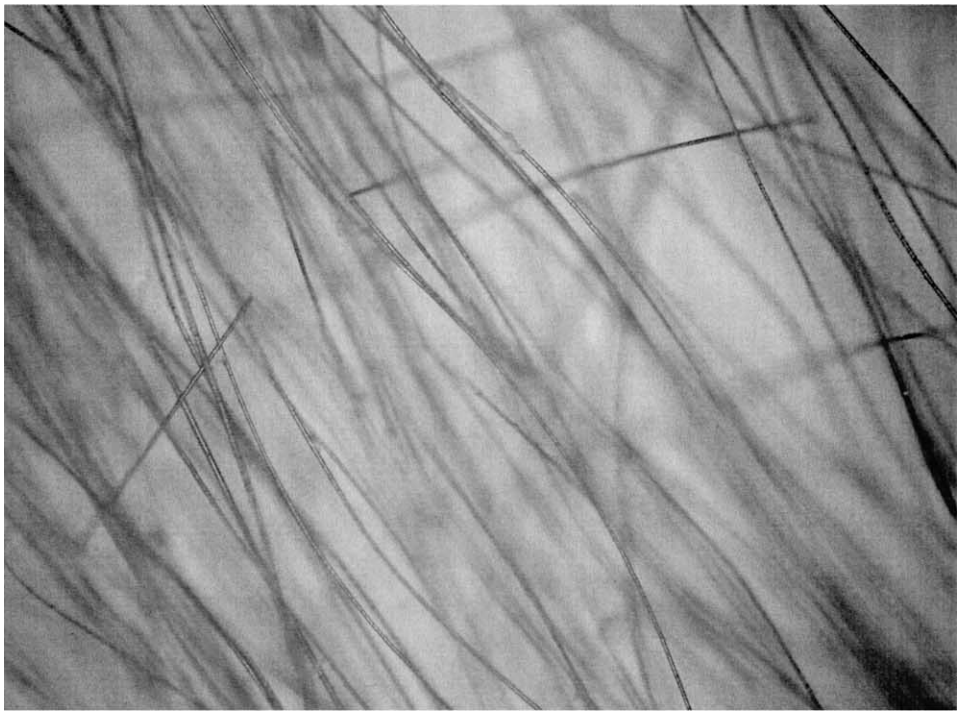

(a)

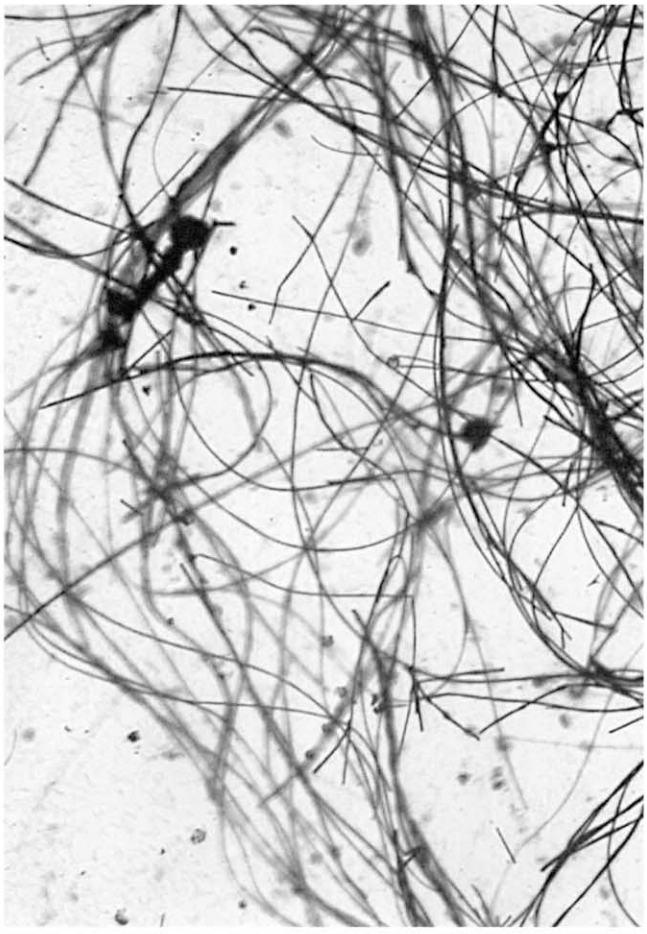

(b)

Fig. 6. Optical micrograph of (a) $GdFeO_3$ gel fibres (b) GdFeO3 fibres heated to 700 °C.

in Fig. 3(b). In this case, the (121) peak intensity is enhanced significantly and the reflections (202) and (240) emerge from the otherwise amorphous background. The fibres crystallise completely on heating at 700 °C, as shown in Fig.3(c). All the prominent reflections corresponding to the perovskite structure for $LaFeO_3$ are clearly seen. It is evident from the interplanar spacing and the relative intensities of diffraction peaks that the fibres are single phase $LaFeO_3$, polycrystalline and randomly oriented. The fibres are free from lattice strain as the XRD reflections did not show any shift in their peak positions. The unit cell parameters calculated from the X-ray diffraction are determined to be $a = 5.552$ Å, $b = 5.563$ Å and $c = 7.862$ Å. These are in agreement with the values reported in the literature [JCPDS 37-1493].

The $SmFeO_3$, $GdFeO_3$, $DyFeO_3$, $ErFeO_3$, and $YbFeO_3$ precursor gel fibres were heated to increasingly higher temperatures, and the XRD patterns were recorded to know the phase composition and determine the unit cell parameters. Fig. 4 gives the XRD patterns of typical orthoferrite fibres heated to 700 °C. It was clear from the XRD results that all the orthoferrite fibres are phase pure and free from additional reflections. The fibres are polycrystalline and did not show any preferential grain alignment. The crystalline orthoferrite phase forms directly without undergoing phase separation into crystalline rare-earth oxide and iron oxide on heating the gel fibres. This suggests that molecular level mixing of metal ions is retained at various stages of processing to enable the formation of perovskite phase at relatively low temperatures.

From the XRD patterns the unit cell parameters were calculated, which are listed in Table 1. As seen from Table 1, the '*a*' and '*c*' parameters decrease for rare-earth ions of smaller size. However, the '*b*' parameter shows only minor variations and it increases slightly in the region La^{3+}–Gd^{3+} but decreases in the region Gd^{3+}–Yb^{3+}. These variations are clearly shown in Fig. 5. These structural variations are the result of the size mismatch between the trivalent rare-earth and Fe^{3+} ions distorting the perovskite lattice to give optimum coordination to Ln ions.[15,16] The Ln–O bond length is enlarged by a cooprative buckling of corner shared FeO_6 octahedra to match Fe–O bond length. The buckling of FeO_6 results in a decreased metal–oxygen–metal bond angle from 180° and the orthoferrites having smaller rare-earth ions adopt the space group Pbnm, whereas, the compounds having larger rare-earth ions crystallize in Pnma.

The photomicrographs of $GdFeO_3$ gel fibres drawn by blow spinning and those heated to 700 °C are shown in Fig. 6(a) and (b), respectively. As seen from the micrographs, the fibres are continuous, and have comparable fibre diameter. The fibres heated to 700 °C were crystalline, adopted perovskite structure, had about 3–4 μm diameter, possessed uneven surface, and they were flexible. Since the samples did not show any clear microstrutural features, they were heated to 1000 °C and higher to induce grain growth. The grain size determined from SEM image was about 0.1 μm for the $GdFeO_3$ fibres heated to 1000 °C. Fig. 7 is the SEM micrograph of a typical single GdFeO3 fibre strand revealing the fibre diameter, surface morphology, and microstructural features.

Fig. 7. SEM micrograph of a single strand of $GdFeO_3$ fibre.

2. Conclusions

The orthoferrite ceramic fibres were successfully produced by a blow spinning process by employing aqueous sols. Nanoparticle dispersions of rare-earth orthoferrite precursors were produced, and combined with a spinning aid (2 wt.% polyethylene oxide) to form a viscous 'spinning solution'. The 'spinning solution' had about about 32±3wt.% solid loading that enabled successful blow spinning. Gel fibres were blow spun, and heated to higher temperatures to convert them to flexible ceramic fibres. The perovskite phase crystallised at relatively low-temperature of 700 °C, and the XRD study revealed crystallinity and phase purity of the fibres. The fibres were polycrystalline, exhibited random grain alignment, and had a diameter of 3–4 μm. The process can be readily scaled up for producing orthoferrite ceramic fibres.

References

1. Shen, S. T. and Weng, H. S., *Ind. Eng. Chem. Res.*, 1998, **37**, 2654.
2. Kharton, V. V., Yaremchenko, A. A., Kovalevsky, A. V., Viskup, A. P., Naumovich, E. N. and Kerko, P. F., *J. Membrane Sci.*, 1999, **163**, 307.
3. Kharton, V. V., Yaremchenko, A. A. and Naumovich, E. N., *J. Solid State Electrochemistry*, 1999, **3**, 303.
4. Kuscer, D., Hrovat, M., Holc, J., Bernik, S. and Kolar, D., *J. Power Sources*, 1996, **61**, 161.

5. Traversa, E., Matsushima, S., Okada, G., Sadaoka, Y., Sakai, Y. and Watanabe, W., *Sensors and Actuators B*., 1995, **25**, 661.
6. Schmool, D. S., Keller, N., Guyot, M., Krishnan, R. and Tessier, M., *J. Appl. Phys*, 1999, **86**, 5712.
7. Sakakima, H., Satomi, M., Hirota, E. and Adachi, H., *IEEE Transactions on Magnetics*, 1999, **35**, 2958.
8. Rajendran, M. and Subba Rao, M., *J. Solid State Chem*., 1994, **113**, 239.
9. Matijevic, E. In *Chemical Processing of Advanced Materials*, ed. L. L. Hench and J. K. West. Wiley, New York, 1992, pp. 513–527.
10. Rajendran, M., Krishna, M. G. and Bhattacharya, A. K., *Thin Solid Films*, 2001, **385**, 230–233.
11. Rajendran, M. and Bhattacharya, A. K., *Mater. Sci. Eng. B*, 1999, **60**, 217.
12. Pullar, R. C., Appleton, S. G., Stacey, M. H., Taylor, M. D. and Bhattacharya, A. K., *J. Mag. Mag. Mater*., 1998, **186**, 313.
13. Pullar, R. C., Appleton, S. G. and Bhattacharya, A. K., *J. Mag. Mag. Mater*., 1998, **186**, 326.
14. Pullar, R. C., Taylor, M. D. and Bhattacharya, A. K., *J. Eur. Ceram. Soc*., 1998, **18**, 1759.
15. Goodenough, J. B. and Longo, J. M., *Magnetic Oxides and Related Compounds, LB new series*. Springer-verlag, New York, 1970.
16. Craik, D. J., *Structure and Properties of Magnetic Materials*. Pion Ltd, London, UK, 1971.